Supporting Information

Confronting Neutrality: Maximizing Success in the Analysis of Transition-Metal Catalysts by MALDI Mass Spectrometry

Gwendolyn A. Bailey and Deryn E. Fogg*

Centre for Catalysis Research & Innovation, Department of Chemistry and Biomolecular Sciences, University of Ottawa, Ottawa, Ontario, Canada K1N 6N5

*Corresponding author. Email: dfogg@uottawa.ca

Table of Contents

S1. Spectrometers and experimental parameters used.

Table S1. MALDI mass spectrometers used, and relevant instrument parameters.

		Laser		
Instrument	**Location**	**Type**	**Wavelength**	**Figure**
AB Sciex 5800 TOF/TOF	MALDI MS / Functional Proteomics Facility, London Regional Proteomics Centre, Western Univ.	Nd:YLF	349 nm	3, S3a
AB Sciex 5800 TOF/TOF	AB Sciex Framingham, MA	Nd:YLF	349 nm	5e
Applied Biosystems 4700 TOF/TOF	MALDI MS / Functional Proteomics Facility, London Regional Proteomics Centre, Western Univ.	Nd:YAG	355 nm	S4a [a]
Applied Biosystems 4800 TOF/TOF	Univ. Toronto Forestry Dept.	Nd:YAG	355 nm	2, 6, 9a
Bruker Microflex TOF	Bruker Daltonics Billerica MA	N_2	337 nm	S3c
Bruker Omniflex TOF	Fogg Anaerobic MALDI-MS Facility, Univ. Ottawa	N_2	337 nm	S3c
Bruker Reflex IV TOF	MALDI MS / Functional Proteomics Facility London Regional Proteomics Centre, Western Univ.	N_2	337 nm	S4b [a]
Bruker Ultraflex II TOF/TOF	Bruker Daltonics Billerica, MA	N_2	337 nm	9b
Bruker UltrafleXtreme TOF/TOF	Bruker Daltonics Billerica, MA	contoured Nd:YAG	355 nm	1, 4, 5a-d, 7, 9c, S1, S2
Shimadzu Performance TOF/TOF	Shimadzu Columbia MD	N_2	337 nm	S3c
ThermoFisher MALDI LTQ Orbitrap XL	Laboratory of Imaging Mass Spectrometry Univ. North Texas	N_2	337 nm	8
Waters Micro MX TOF	Advanced Instrumental Mass Spectrometry Lab Univ. Toronto	N_2	337 nm	S3c
Waters Synapt G2-Si MALDI-QTOF	Waters Corp. Milford MA	Nd:YAG	355 nm	S3b

[a] At the time of use, these lasers were near the end of their operational lifetimes, and higher applied laser energies were therefore required. The impact on fragmentation is illustrated in Fig. S4.

S2. Additional examples showing impact of matrix ε_M on fragmentation.

These spectra supplement the two extremes shown in Figure 4.

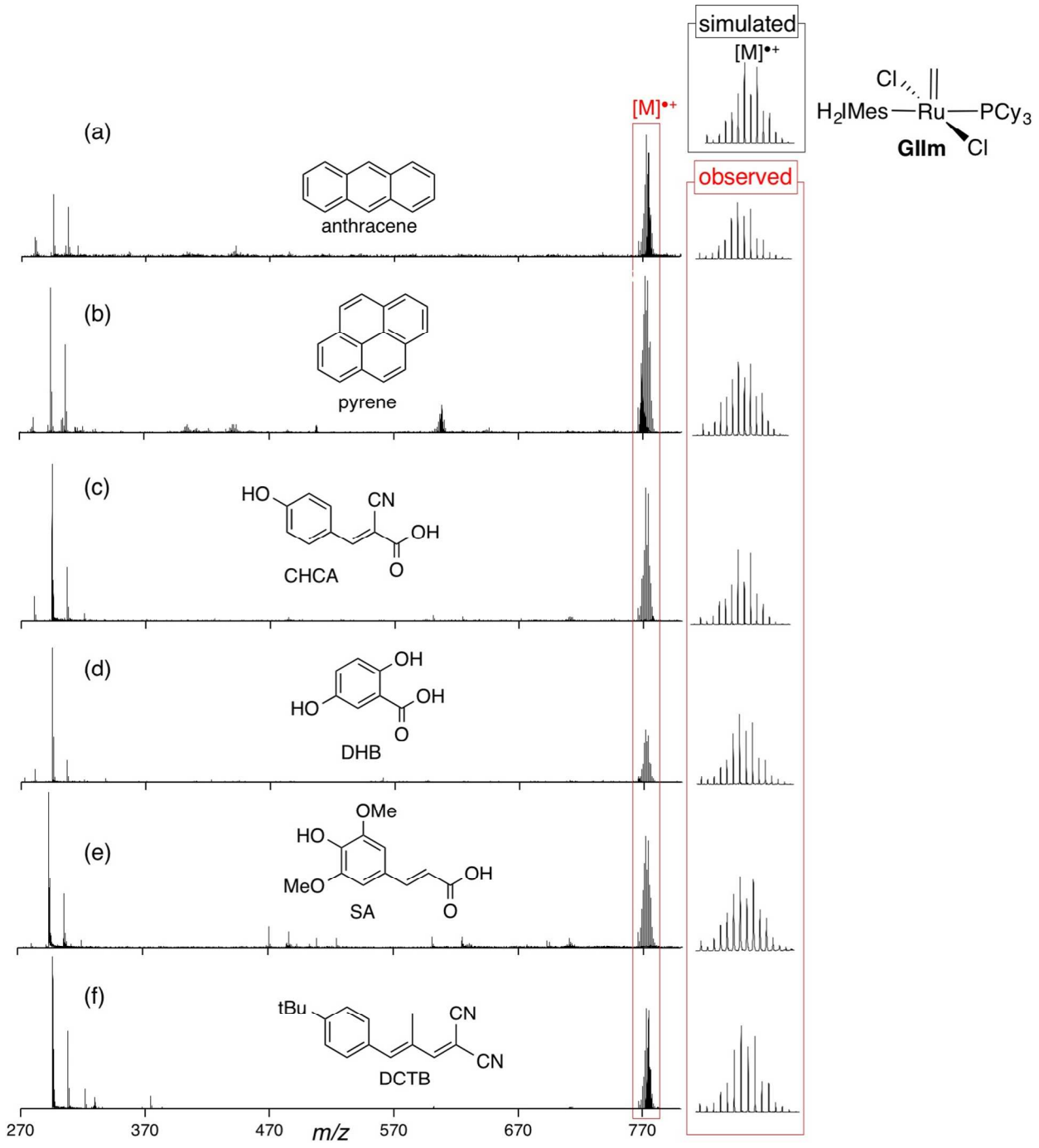

Figure S1. Impact of matrix ε_M on fragmentation, assessed in analysis of non-labile **GIIm.** MALDI mass spectra of **GIIm** with (a) anthracene; (b) pyrene; (c) CHCA; (d) DHB; (e) SA; (f) DCTB.

S3. Spectra showing aggressive decomposition by functionalized matrices.

These examples supplement the spectra shown in Figure 5, which focus on more widely-used matrices.

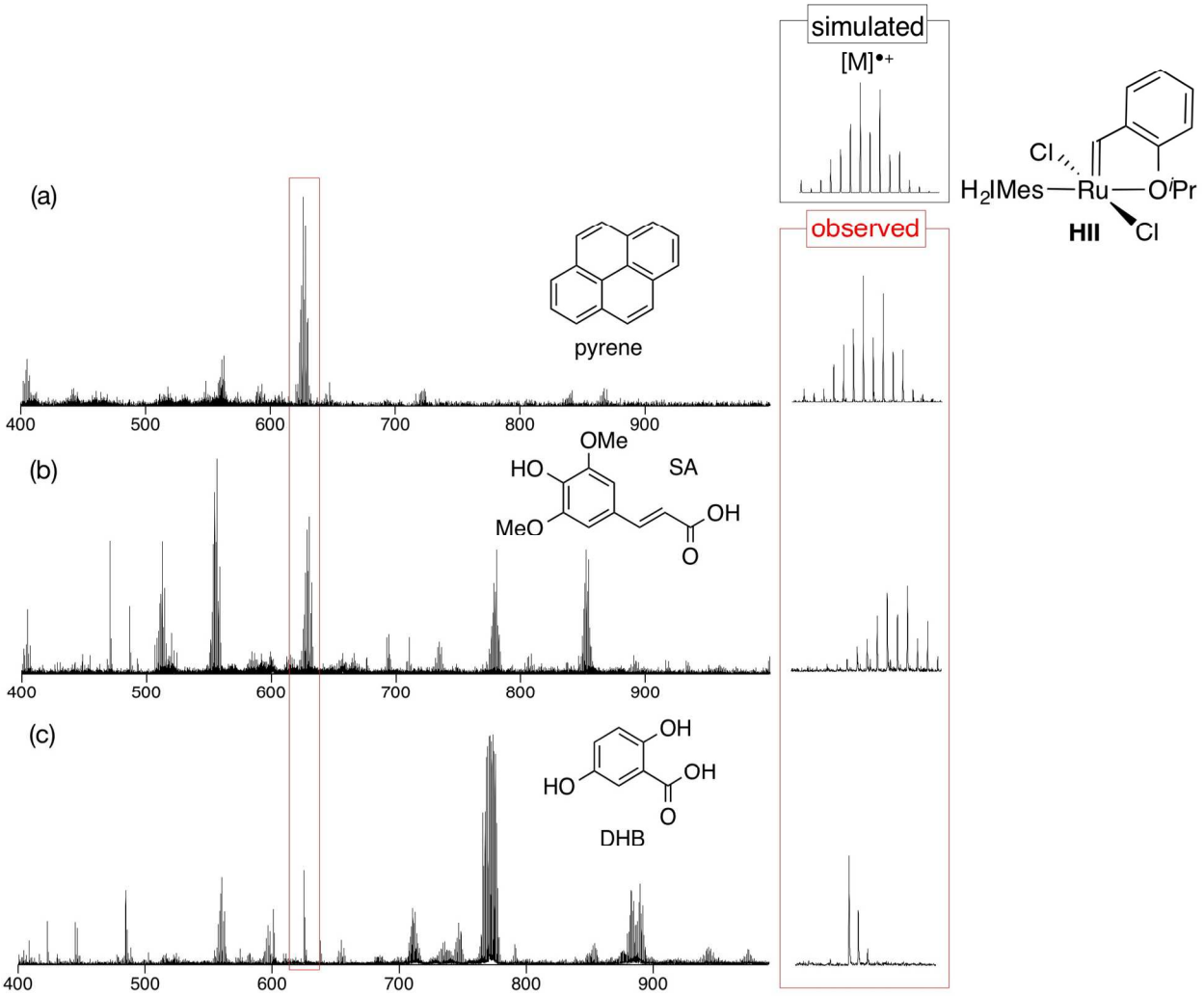

Figure S2. MALDI mass spectra showing gas-phase decomposition of **HII** by functionalized matrices, as compared to the benchmark pyrene. (a) Pyrene; (b) SA; (c) DHB.

S4. Spectra showing impact of laser beam profile on fragmentation.

These examples supplement the spectra shown in Figure 9 (which were drawn from instruments matched as closely as possible, to facilitate comparison).

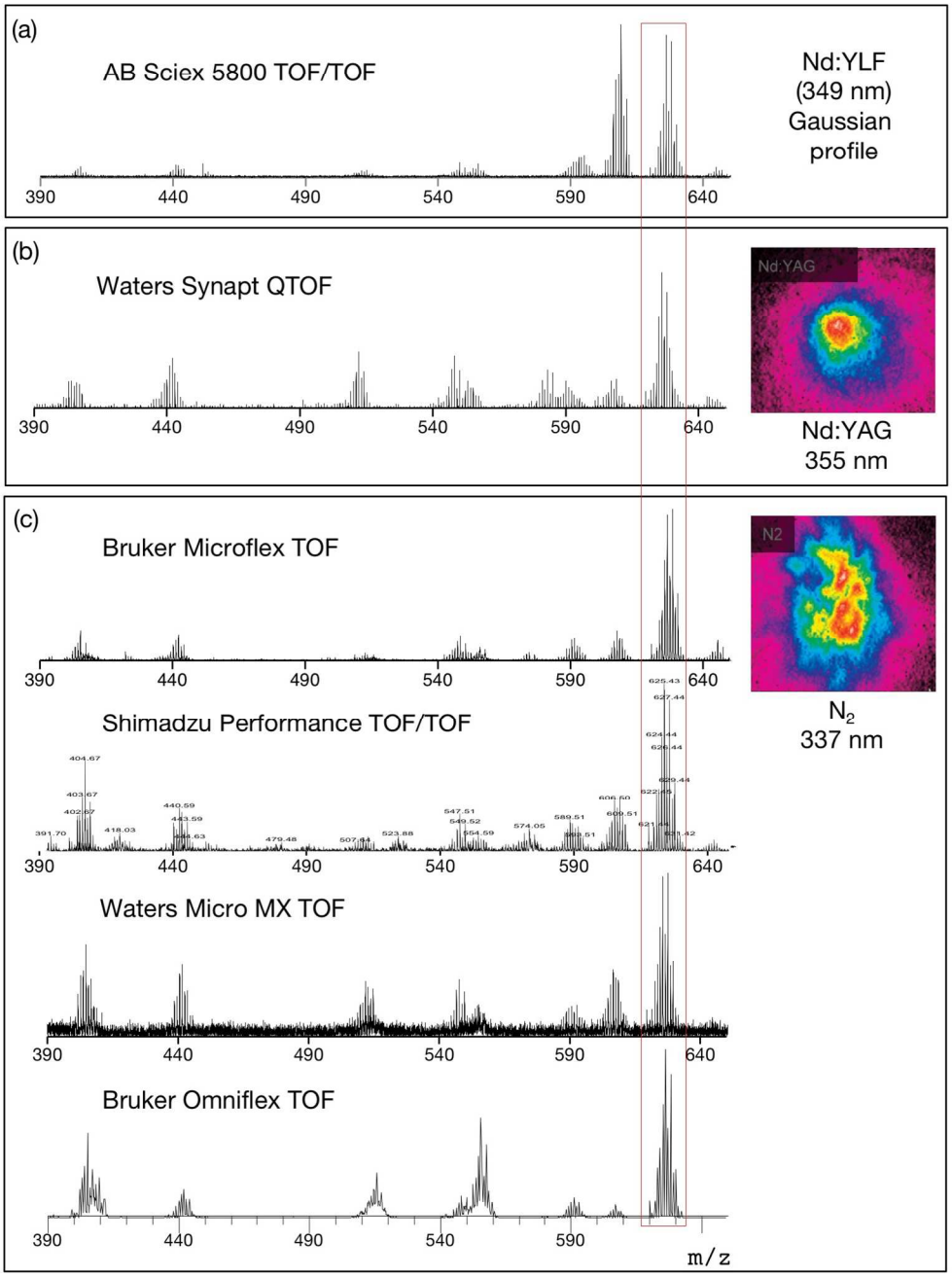

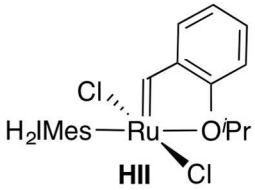

Figure S3. Impact of laser beam profile on fragmentation of **HII**. Spectra recorded using (a) a Nd:YLF laser; (b) a Nd:YAG laser; and (c) a N_2 laser.

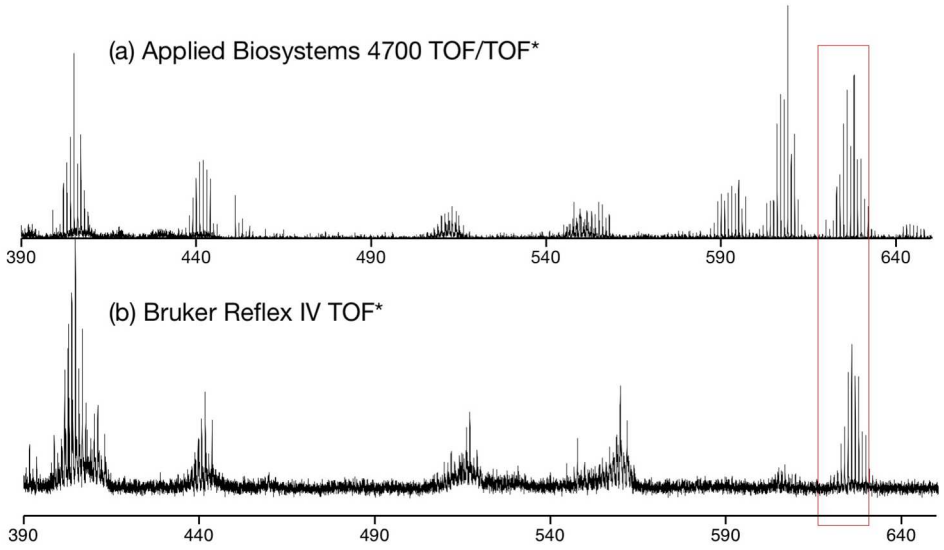

Figure S4. Negative impact of laser age on performance. MALDI mass spectra recorded for **HII** on (a) Nd:YAG (Applied Biosystems 4700) and (b) N_2 (Bruker Reflex II) lasers that were nearing the end of their lifetime, necessitating use of higher applied laser energies.

S5. UV-vis spectra of selected matrices and analytes.

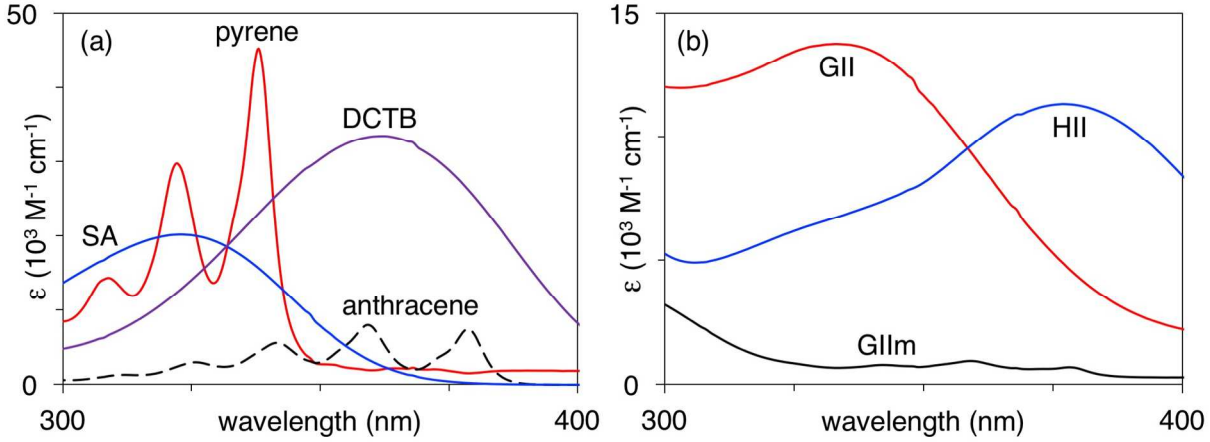

Figure S5. (a) UV-vis spectra of the matrices pyrene, anthracene, and DCTB in CH_2Cl_2; spectrum of SA (which is very poorly soluble in CH_2Cl_2) in methanol. (b) UV-vis spectra of the analytes **GII**, **GIIm**, and **HII** in CH_2Cl_2.